



Evaluation and improvement study of the Planetary Boundary-Layer schemes during a high PM_{2.5} episode in a core city of BTH region, China

Jianbo Yang ^{a,b,c}, Yingxiao Tang ^c, Suqin Han ^{c,*}, Jingle Liu ^{a,b}, Xu Yang ^c, Jian Hao ^{a,b}

^a Tianjin Key Laboratory for Oceanic Meteorology, Tianjin 300074, China

^b Tianjin Institute of Meteorological Science, Tianjin 300074, China

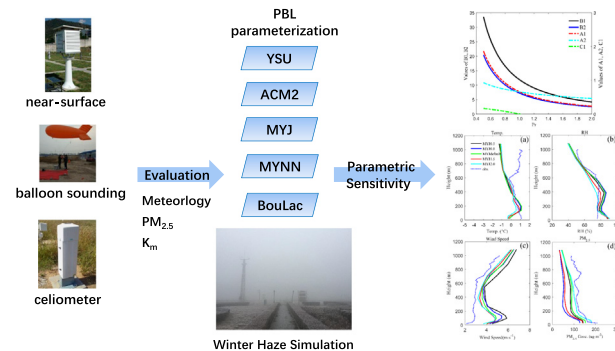
^c CMA-NKU Cooperative Laboratory for Atmospheric Environment-Health Research, Tianjin 300074, China



HIGHLIGHTS

- Impacts of 5PBL schemes on vertical profiles of PM_{2.5}/turbulence are examined.
- Vertical distribution of observed Km is derived to directly evaluate the PBL scheme.
- MYJ fails to distinguish the turbulent intensity between different pollution stages.
- A new set of MYJ parameters is recommended to improve the winter haze simulation.

GRAPHICAL ABSTRACT



ARTICLE INFO

Article history:

Received 30 July 2020

Received in revised form 21 September 2020

Accepted 28 September 2020

Available online 16 October 2020

Editor: Pingqing Fu

Keywords:

PBL parametrization

WRF-Chem model

Vertical profile

Haze simulation

Parametric sensitivity

Turbulent Prandtl number

ABSTRACT

Accurate depictions of planetary boundary layer (PBL) processes are important for both meteorological and air quality simulations. This study examines the sensitivity of the model performance of the Weather Research Forecasting model coupled with Chemistry (WRF-Chem) to five different PBL schemes and further to different turbulence parameters for the simulation of a winter haze episode in Tianjin, a core city of the Beijing-Tianjin-Hebei (BTH) region in China. To provide a direct and comprehensive evaluation of the PBL schemes, measurements from multiple instruments are employed, including both meteorological and air quality quantities from near-surface observations, vertical sounding measurements and ceilometer data. Moreover, the vertical distribution of the turbulent exchange coefficient is derived from sounding measurements and is utilized to evaluate the PBL schemes. The results suggest that the Mellor-Yamada-Janjic (MYJ) scheme is generally statistically superior to the other schemes when comparing observations. However, considerable model discrepancies still exist during certain stages of this haze episode, which are found to be predominantly due to the deficiency of MYJ in distinguishing the intensity of turbulent mixing between different pollution stages. To improve the model performance, this study further tests the impact of different closure parameters on the simulation of winter haze episode. In the MYJ scheme, the closure parameters play a key role in the turbulent mixing within the PBL and therefore in haze simulations. Sensitivity experiments with different MYJ parameters confirm this diagnosis and suggest that a larger Prandtl number (Pr), rather than the default value in the MYJ formulation, may be more applicable for haze simulations under stable atmospheric conditions.

© 2020 Elsevier B.V. All rights reserved.

* Corresponding author.

E-mail address: sq_han@126.com (S. Han).

1. Introduction

With the booming economic development and urbanization processes, air pollution in the Beijing, Tianjin and Hebei (BTH) region of China has attracted wide concern from both the public and government (Lee et al., 2015; Qi et al., 2017; Yang et al., 2019). During severe haze episodes, the instantaneous PM_{2.5} concentration usually reaches hundreds of $\mu\text{g m}^{-3}$ in this region (Zheng et al., 2016). Tianjin is one of the core cities in the BTH region and is also a severely polluted city. Previous studies have examined the vertical distribution of haze episodes in Tianjin based on a 255 m tower (Zhang et al., 2011; Tian et al., 2013). Han et al. (2018) conducted an intensive field campaign to observe the vertical distribution of meteorological parameters and PM_{2.5} during a typical winter haze episode in Tianjin. The substantial downward transportation of regional pollution from high atmospheric layers and stagnant weather conditions within the planetary boundary layer (PBL) are recognized as the key factors in the emergence of haze episodes. PBL is the lowest part of the atmosphere and is where meteorological conditions and air pollutants directly affect human activities. Turbulent diffusion is an important indicator for characterizing the vertical structure of PBL, hence affects the transport and dispersion of air pollutants (Xie et al., 2012). The intensity of turbulent diffusion strongly determines the level of haze pollutions (Wang et al., 2018).

Numerical models (e.g., the WRF-Chem model) are commonly recognized as robust tools for the analysis and forecast of air quality issues (Grell et al., 2005; Fast et al., 2006). Nonetheless, evident discrepancies still exist between the observed and modeled meteorological fields as well as pollutant concentrations, especially during severe air pollution episodes (Wang et al., 2018; Li et al., 2016). One substantial source of forecast uncertainties in mesoscale meteorological and air quality models is the representation of the thermodynamic and kinematic structures within the PBL (Han et al., 2008; Cohen et al., 2015).

The PBL parameterization scheme is responsible for depicting the vertical profiles of sub-grid fluxes due to eddy transport in the atmosphere. It plays an important role in the exchanges of mass, moisture and energy between land (ocean) and atmosphere, hence could affect the model performance of meteorology and air quality to a large extent (Garratt, 1994; Chaouch et al., 2017). A number of PBL parameterization schemes have been developed to depict the turbulent processes in mesoscale numerical models (Mellor and Yamada, 1982; Hong et al., 2006; Pleim, 2007). At present, there has been considerable uncertainty in the estimations of the vertical mixing in the PBL (Ha and Mahrt, 2001; Avolio et al., 2017; Tymvios et al., 2018). Several studies have examined the sensitivity of Weather Research and Forecast (WRF) model predictions to different PBL schemes (Hu et al., 2010; Roman-Cascon et al., 2012; Steeneveld et al., 2015). The optimum selection and performance of different PBL schemes strongly depends on the parameters concerned, geographical and climatological features of the study area, and time of year (Ruiz et al., 2010; Banks et al., 2016).

Researches focusing on the performance of WRF-Chem with respect to different PBL schemes are relatively few (Fountoukis et al., 2018; Mohan and Gupta, 2018). Banks and Baldasano (2016) investigated the impacts of four PBL schemes on simulations of PBL height (PBLH), surface pollutant concentrations, and surface and upper-air meteorological variables. Chen et al. (2017) conducted a sensitivity study of WRF-Chem with different PBL schemes to identify the optimum configuration for simulating near-surface meteorological observations and PM_{2.5} concentrations during an extreme high PM_{2.5} episode in Beijing. The above studies have all focused on the assessment of model performance near the surface, and few have addressed the prognostic capability in reproducing vertical profiles of pollutant concentrations. However, the vertical structure of the PBL plays a critical role and hence should be fully considered in the studies of model evaluation and improvement (Hu et al., 2013).

PBL schemes always utilize multiple parameters or empirical constants for turbulence parameterization. For example, closure

parameters determine the relative proportions of different turbulence length scales to the master turbulence length scale. Different selection of these parameters may alter the vertical structure of PBL physical or chemical properties by changing the vertical mixing of turbulence (Nielsen-Gammon et al., 2010). Pr can be viewed as a ratio that reflects the eddy diffusivity of momentum to that of heat and governs the strength of turbulent mixing (Schlichting, 1979). A global study showed that reducing the value of Pr from unity to 0.8 would warm and moisten the lower part of the PBL and reduce some long-standing model biases in stratocumulus regions. Li (2019), in a recently published review, indicated that studies concerning the role of Pr in weather and atmospheric chemistry models are surprisingly sparse and that more studies are needed to systematically investigate the sensitivity of simulation results to the selection of Pr .

In summary, although several researches have discussed the performance of different PBL schemes, there are still some challenges. First, model evaluations of WRF-Chem with respect to different PBL schemes are relatively few and most of these works have only indirectly evaluated PBL schemes through comparisons against near-surface observations. Research effort should be conducted to collect observation data in vertical profiles of both meteorological and air quality factors, to allow a direct and comprehensive evaluation of PBL schemes (Parra, 2019). Second, the existing PBL schemes still need further modification and improvement studies for accurate descriptions of extreme haze events, but until now, little relevant work has been conducted beyond the work of the original authors (An et al., 2007). Jahn et al. (2017) demonstrated the potential for improving the performance of wind forecasts through parameter modification in the MYNN (Mellor-Yamada-Nakanishi-Niino) scheme. Xu et al. (2015) examined the impact of different mixing coefficients on rainfall simulations over the lower Yangtze River Valley. The above studies have only identified the sensitivity of meteorological models to PBL parameters, while the impact of such parameters on air quality predictions should also be identified.

The aims of the present study are to (1) investigate the sensitivity of both meteorological and chemical variables to five different PBL schemes over coastal urban underlying surfaces in Tianjin, a core city of the BTH region, China; (2) evaluate the sensitivities of WRF-Chem simulations to the turbulent closure parameters (A_1, A_2, B_1, B_2, C_1) in the MY scheme; and (3) modify the values of these PBL parameters to improve the model capacity in better characterizing severe haze events. The remainder of this paper is organized as follows. In Section 2 the WRF-Chem model configuration and experimental design as well as the multiple observation data employed in this study are described in detail. Section 3 evaluates the impacts of different PBL parameterization schemes on the model performance of WRF-Chem and find the optimum one for simulating both the meteorological and air quality fields during winter haze days in Tianjin. Moreover, Section 3 also investigates the model sensitivity to different sets of turbulence parameters in order to find the most suitable parameters for model simulations under winter haze conditions. Finally, a brief summary is given in Section 4 as a conclusion.

2. Methodology

2.1. Model configuration

In the present study, a three dimensional meteorology-chemistry model, WRF-Chem version 3.8.1, is applied to investigate the sensitivity of PBL schemes in simulating meteorological and chemical variables during a severe haze episode in Tianjin. The WRF-Chem model has been proved to be a robust tool in simulating meteorological fields and air quality from city-scales to meso-scales in China (Li et al., 2011; Tie et al., 2013).

Three model domains with two-way nesting are employed in the simulation with grid resolutions of 27 km, 9 km and 3 km, respectively (Fig. 1). The horizontal grid dimensions for each domain are 119×115 ,

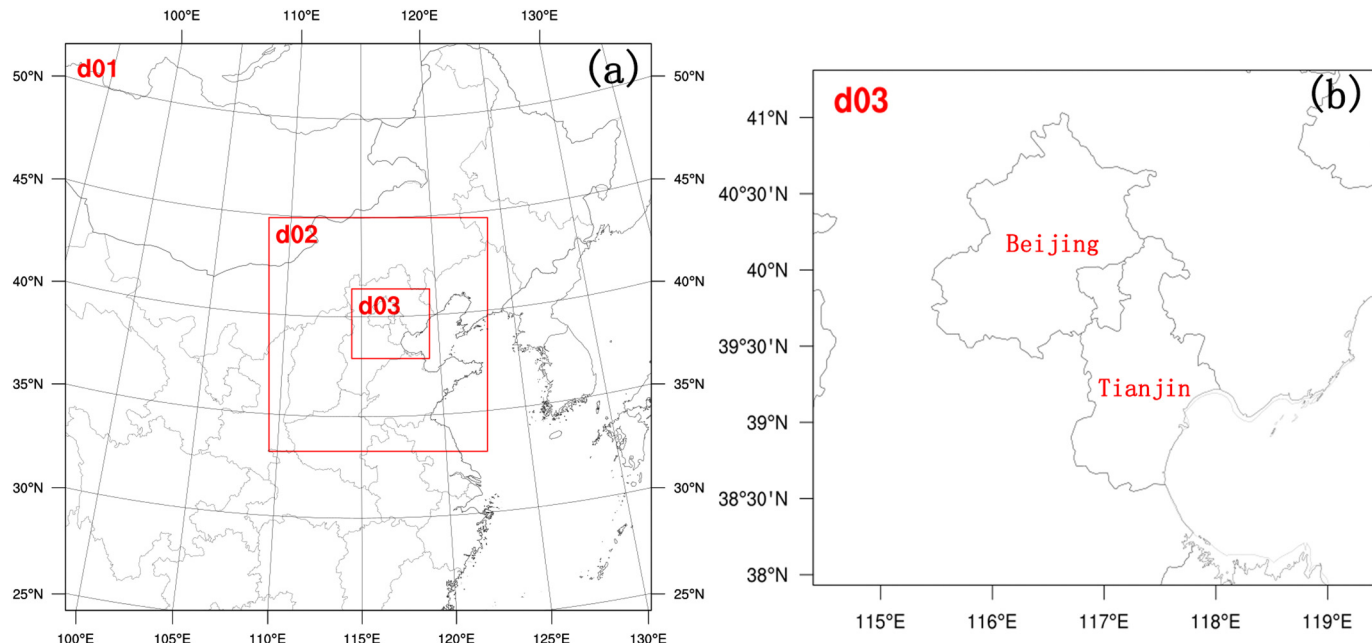


Fig. 1. (a) Three nested modeling domains for sensitivity simulations and (b) the innermost domain.

133 × 142 and 142 × 127, respectively. The largest domain (d01) covers most of eastern and northern China and is centered at 39.64°N, 116.91°E. The intermediate domain (d02) contains the entire BTH region and its upstream areas including Shanxi, Shandong, Henan and Inner Mongolia provinces. The finest domain (d03) covers the two largest megacities within the BTH region, namely Beijing and Tianjin. The vertical structure is divided into 30 levels, of which 10 layers are lower than 1 km and the lowest level is approximately 20 m above the ground level. The simulation period runs from 00:00 UTC 24th December 2017 to 00:00 UTC 3rd January 2018, covering a severe PM_{2.5} pollution episode that occurred in the BTH region. The first 12-h is considered to be the simulation spin-up time. The physics schemes used in this study are as follows: the WRF single-Moment 5-class scheme for microphysics, the Goddard shortwave scheme for shortwave radiation and the RRTM scheme for longwave radiation, the Grell 3D scheme for cumulus parameterization, and the Noah Land Surface Model coupled with the Single Layer Urban Canopy Model is chosen as the urban surface scheme. The initial and boundary conditions are obtained from the National Center for Environmental Prediction (NCEP) Final Analysis (FNL) data with a spatial resolution of 1° × 1° and temporal resolution of 6 h. For major chemical options, the gas-phase chemistry module RADM2 (Stockwell et al., 1990) and the aerosol module MADE/SORGAM (Schell et al., 2001) are employed in this study. The Multi-resolution Emission Inventory of China (MEIC) (<http://www.meicmodel.org/>) is employed as the anthropogenic emission input of the chemistry module (Qi et al., 2017).

Five PBL parameterization schemes are adopted in the model runs to compare the simulation results of meteorological and chemical

variables under heavy haze pollution conditions in Tianjin. An overview of these five PBL schemes is shown in Table 1.

2.2. Observational data

To allow a direct and comprehensive assessment of the PBL schemes, multiple sources of observation data are collected in vertical profiles, as well as surface measurements, of meteorological and air quality quantities.

During the air pollution episode in the winter of 2017, an intensive field campaign was conducted in the urban center of Tianjin (39°04' N, 117°12' E) and Hangu District (39°10' N, 117°48' E). Hangu is a coastal area located at the eastern edge of the BTH area. To obtain a full picture of the vertical structure of the urban boundary layer, all parameters were synchronously measured during this episode.

2.2.1. Tethered balloon

In order to directly obtain vertical profiles of PM_{2.5} and the meteorological parameters throughout the PBL (approximately 0–1 km), an intensive field campaign was conducted using a tethered balloon during the haze episode. The tethered balloon platform consisted of two major components. The jet-shaped tethered balloon acted as a carrier and was filled with 6.5 m³ of helium gas, which allowed a maximum payload of 5.0 kg. The monitoring instruments, which measured meteorological parameters (temperature, humidity, horizontal wind speed and direction sensors) and particle mass concentrations (TEMO Mie pDR-1500), were mounted underneath the balloon. The tethered balloon was scheduled to be launched 6 times a day (namely, 05:00,

Table 1

Descriptions of the five WRF PBL schemes employed in this study, including long name, turbulent kinetic energy closure type, operational method and threshold value for diagnosing PBL height, and corresponding references.

Long name	Closure order	PBL height method	Threshold	Reference
YSU	Yonsei University	1.0 non-local	Ri _b calculated from surface 0 (unstable) 0.25 (stable)	Hong et al. (2006)
ACM2	Asymmetric Convective Model v2	1.0 non-local	Ri _b calculated above neutral buoyancy level 0.25	Pleim (2007)
BouLac	Bougeault-Lacarrère	1.5 local	TKE-prescribed threshold $5.0 \times 10^{-3} \text{ m}^2 \text{ s}^{-2}$	Bougeault and Lacarrère (1989)
MYJ	Mellor-Yamada-Janjic	1.5 local	TKE-prescribed threshold $0.2 \text{ m}^2 \text{ s}^{-2}$	Janjic (2002)
MYNN2.5	Mellor-Yamada-Nakanishi-Niino Level 2.5	1.5 local	TKE-prescribed threshold $1.0 \times 10^{-6} \text{ m}^2 \text{ s}^{-2}$	Nakanishi and Niino (2006)

08:00, 14:00, 17:00, 20:00 and 23:00 LST) when wind speeds permitted ($\leq 8 \text{ m s}^{-1}$). It was launched to ascend at a steady speed of 0.5 m s^{-1} until reaching a maximum height of 1000 m, remained at the maximum height for approximately 5 min, and then descended at the same rate. Unfortunately, vertical profiles at the end of this haze episode cannot be obtained due to the unfavorable weather.

2.2.2. Synchronous ground-based observation

Surface meteorological parameters and air pollutant concentrations were synchronously measured at a nearby measurement site of the Hangu meteorological bureau. In addition, vertical gradient observations of the meteorological parameters, turbulence data and PM_{2.5} mass concentrations from the ground to upper levels were obtained from a 255 m meteorological tower. The meteorological tower is located at the urban boundary layer observation station (WMO Id. No.54517, 39°04' N, 117°12' E) of Tianjin, China. The meteorological parameters, including temperature, horizontal wind speed, wind direction and relative humidity, were measured at 15 platform heights (5, 10, 20, 30, 40, 60, 80, 100, 120, 140, 160, 180, 200, 220 and 250 m) of the tower every 10 s, and hourly-averaged data were adopted in the present study. CAST-3 three dimensional ultrasonic anemometers (Campbell Scientific, Inc., USA) were installed at 40, 120 and 200 m to measure the turbulence data. These meteorological and turbulence data are important for describing variations within the PBL.

Furthermore, the vertical PBL structure and its height (PBLH) were also monitored with a ceilometer (CL31, VAISALA) during the campaign. This instrument measured the total aerosol backscatter coefficient every 10s with a vertical resolution of 20 m and height range within 20–7500 m. Since aerosol concentrations are generally lower in the free atmosphere, PBLH observations could be identified by the large gradients in the vertical backscattering profile.

2.2.3. Quality control

To assure the quality and reliability of the observation data, all deployed instruments were examined thoroughly and calibrated before the beginning of the field campaign. Furthermore, pairs of instruments were employed to continuously measure the PM_{2.5} mass concentration on the ground and the measured data were inter-compared. The result is exhibited in Fig. 2, and a linear regression was fitted, which indicated that TEMO Mie pDR-1500 could be applied in the vertical sounding observation.

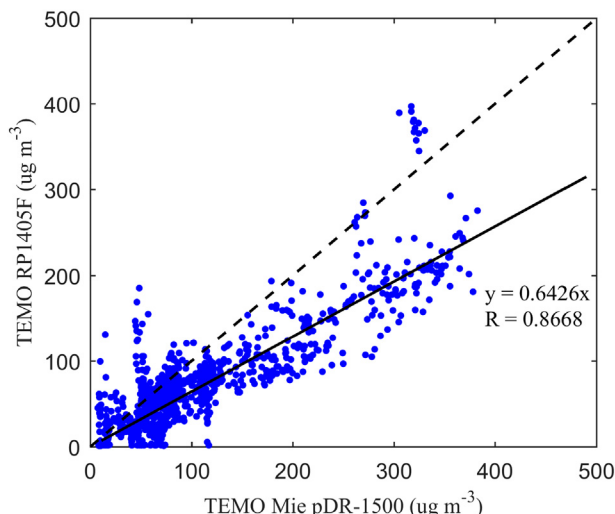


Fig. 2. Comparison of PM_{2.5} concentrations measured by TEMO Mie pDR-1500 and RP1405F.

2.3. Statistics metrics for model evaluation

The simulated surface and vertical profiles of meteorological variables (e.g., temperature, relative humidity, and wind speed) and PM_{2.5} concentration are compared with the corresponding observation data to evaluate the performance of WRF-Chem during the studied haze episode. The statistics metrics adopted in the present study included the mean bias (MB), mean absolute bias (MAB), root mean square error (RMSE), correlation coefficient (R) and index of agreement (IOA), which are defined as follows:

$$\text{MB} = \frac{1}{n} \sum_{i=1}^n (m_i - o_i) = \bar{m} - \bar{o} \quad (1)$$

$$\text{MAB} = \frac{1}{n} \sum_{i=1}^n |m_i - o_i| \quad (2)$$

$$\text{RMSE} = \sqrt{\frac{1}{n} \sum_{i=1}^n (m_i - o_i)^2} \quad (3)$$

$$R = \frac{\sum_{i=1}^n (m_i - \bar{m})(o_i - \bar{o})}{\sqrt{\sum_{i=1}^n (m_i - \bar{m})^2} \sqrt{\sum_{i=1}^n (o_i - \bar{o})^2}} \quad (4)$$

$$\text{IOA} = 1 - \frac{\sum_{i=1}^n (m_i - o_i)^2}{\sum_{i=1}^n (|m_i - \bar{o}| - |o_i - \bar{o}|)^2} \quad (5)$$

where o_i is the observation, m_i is the modeled result, and n is the number of samples.

2.4. Experimental design for modification of turbulence-related parameters

In the MYJ scheme, the closure parameters (A_1, A_2, B_1, B_2, C_1) are the proportional coefficients of the turbulence length scales and the master turbulence length scale, which could finally affect turbulent mixing within the PBL. The equations for the closure coefficients are interconnected as follows (Janjic, 2002):

$$A_1 = B_1 \frac{1-3\gamma_1}{6}, \quad (6)$$

$$A_2 = \frac{1}{3\gamma_1 B_1^{1/3} Pr}, \quad (7)$$

Table 2

A summary of numerical experiments based on different values of Pr in the MYJ PBL scheme.

Experiments	Value of Pr	(A_1, A_2, B_1, B_2, C_1)
MYJ0.5	0.5	$A_1 = 1.866446574$ $A_2 = 0.929842605$ $B_1 = 33.59603833$ $B_2 = 20.44096308$ $C_1 = 0.166874406$
MYJ0.8	0.8	$A_1 = 0.922222235$ $A_2 = 0.73508785$ $B_1 = 16.60000023$ $B_2 = 10.10000014$ $C_1 = 0.080531812$
MYJdefault	1.0 (Default value)	Default values of the original MYJ PBL scheme
MYJ1.5	1.5	$A_1 = 0.359197811$ $A_2 = 0.53681539$ $B_1 = 6.465560591$ $B_2 = 3.933865179$ $C_1 = -0.275908127$
MYJ2.0	2.0	$A_1 = 0.233305822$ $A_2 = 0.464889078$ $B_1 = 4.199504791$ $B_2 = 2.555120385$ $C_1 = -0.663342843$

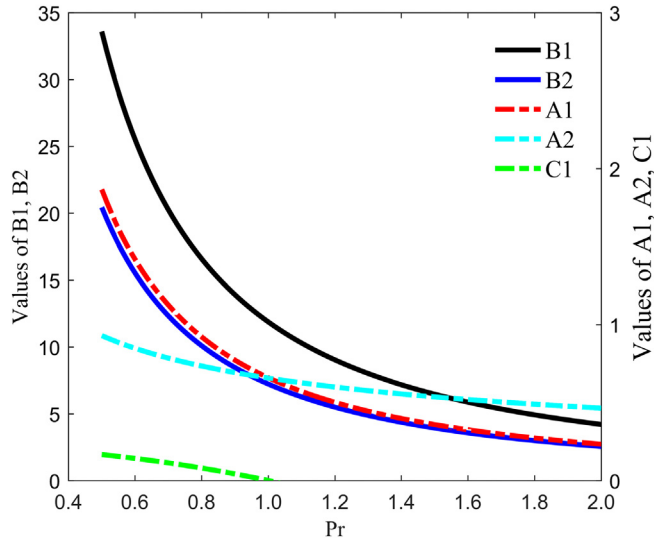


Fig. 3. Variations of the turbulent closure parameters (A_1, A_2, B_1, B_2, C_1) as a function of Prandtl number.

$$B_1 = \left[\left(R_B F_B^2 \right) / \text{Pr} \right]^{3/2}, \quad (8)$$

$$B_2 = \frac{B_1}{R_B}, \quad (9)$$

$$C_1 = \gamma_1 - \frac{1}{3A_1 B_1^{1/3}} \quad (10)$$

where Pr is the turbulent Prandtl number, R_B and F_B are constants whose values are supposed in Janjic (2002). Therefore, the determination of the closure parameters (A_1, A_2, B_1, B_2, C_1) will be made by the choice of Pr (Table 2). The original Pr value is set to 1.0 according to Janjic (2002). It can be concluded that the model performance of WRF-Chem is related to the closure parameters and hence the selection of Pr . Of interest here is whether the default value of Pr , which was determined from classical neutrally stratified laboratory measurements, is suitable for modeling the haze events in winter and the influence of different Pr values on the simulation of winter haze episodes remains unknown. In the present study, we would investigate the impact of Pr on the performance of the WRF-Chem model.

The Pr value was estimated to be within the range between 0.7 and 1.2 under neutral or weakly stable conditions (Schumann and Gerz, 1995), whereas a range of 0.5–2 was inferred according to Kim and Mahrt (1992). Grachev et al. (2007) concluded that the upper limit of Pr should be 2 or 3. Based on a review of the existing literature, a range of 0.5–2 was employed for Pr in the present study. Consequently, we choose values of 0.5, 0.8, 1.0, 1.5, 2.0 for Pr , respectively, to conduct numerical experiments (see Table 2) for the purpose of assessing the role of Pr in winter haze simulations. On the basis of Eqs. (6)–(10), we obtain the corresponding values of the closure parameters in the MYJ PBL scheme (Table 2). Fig. 3 exhibits the variation tendencies of the parameters (A_1, A_2, B_1, B_2, C_1) with Pr . Both B_1 and B_2 change greatly with Pr , whereas A_1, A_2 and C_1 vary slightly. The Pr is a function of the PBLH and the M-O length scale (Noh et al., 2003). The PBLH reflects the turbulence strength within the PBL and the M-O length scale is related to atmospheric stability. Hence the turbulent length scales, B_1 and B_2 , change a lot due to the variations of turbulent motion and atmospheric stability. Conversely, changes of B_1 and B_2 would also induce significant effects on the mixing capacity of atmospheric turbulence.

3. Results and discussions

3.1. Overview of the haze pollution episode

The time series of the $\text{PM}_{2.5}$ mass concentrations in Tianjin during this haze episode are shown in Fig. 4. Additionally, Fig. 5 shows the synchronously measured vertical distribution of temperature, relative humidity and wind based on the 255 m meteorological tower in Tianjin.

For further analysis, the evolution of this episode is divided into four stages: (1) The primary stage (Stage 1) was before 0900 LST on December 27, 2017. An easterly wind continued to blow near the surface at a speed of 1.0–2.0 m s^{-1} . The surface temperature ranged between –2 and 1 °C and no clear temperature inversion occurs. The air quality at this stage was quite good with an average $\text{PM}_{2.5}$ concentration lower than $20 \mu\text{g m}^{-3}$. (2) The rapid formation stage (Stage 2) was from 0900 LST December 27 to 0200 LST December 29. The $\text{PM}_{2.5}$ concentration increased sharply from 20 to $190 \mu\text{g m}^{-3}$ during this period. The wind turned southerly on December 28 with lower speeds of 0.5–1.0 m s^{-1} and the air became moister (relative humidity reached 90%). Both the moister air and lower winds favor the elevation of the $\text{PM}_{2.5}$ concentrations through hygroscopic growth and pollution accumulation. (3) The maintenance stage (Stage 3) was from 0200 LST

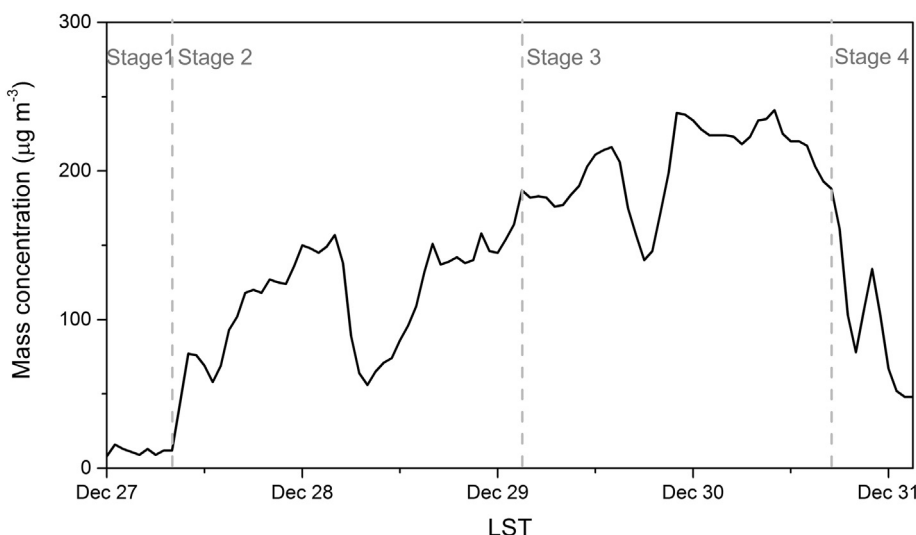


Fig. 4. Time series of $\text{PM}_{2.5}$ mass concentration in Tianjin and the stage division of this pollution episode.

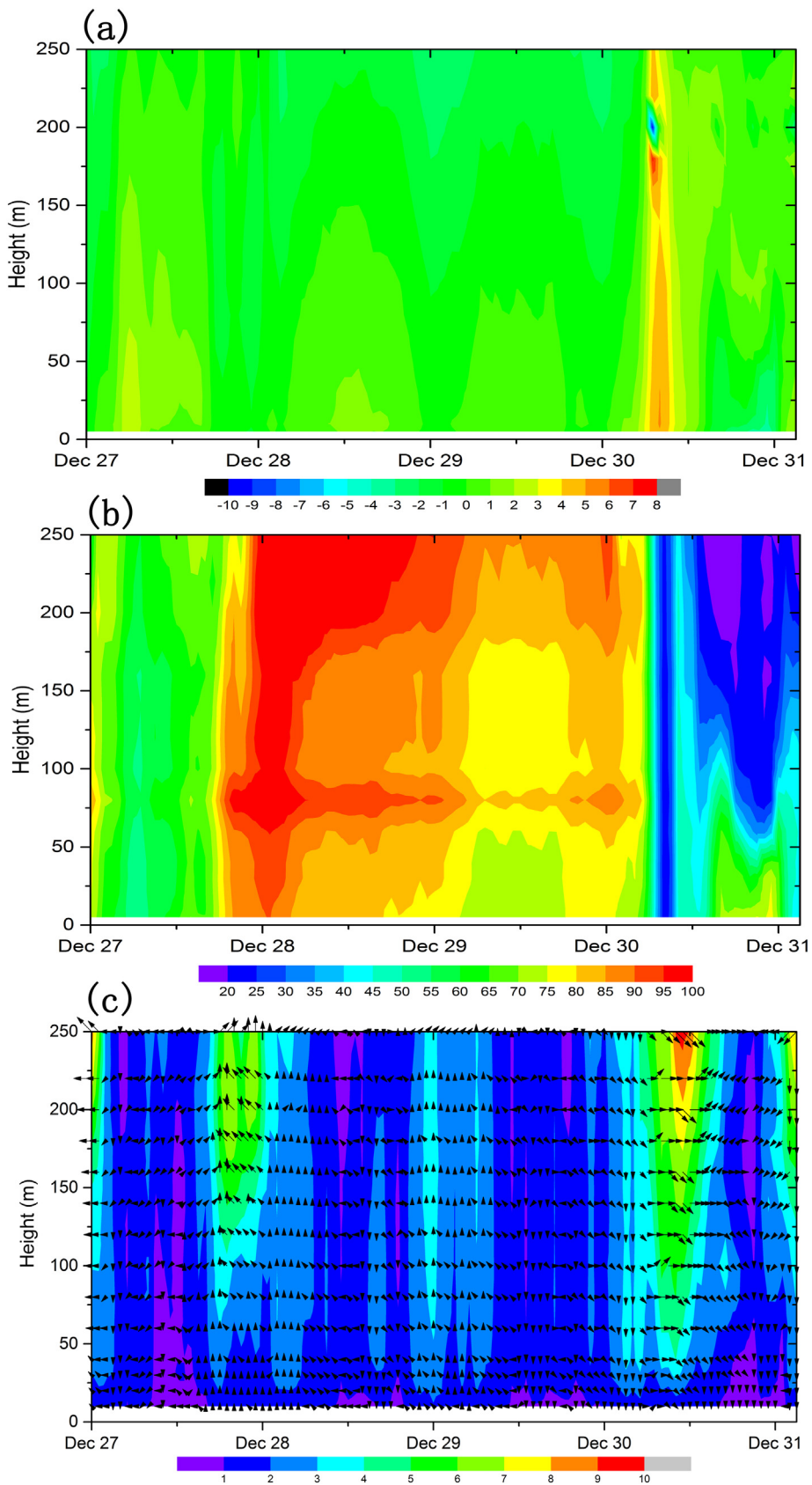


Fig. 5. Vertical distribution of wind vector (a), relative humidity (b) and air temperature (c) during the haze episode.

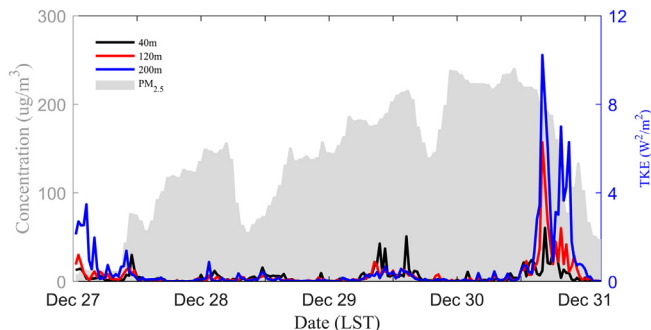


Fig. 6. Time variations of turbulent kinetic energy (TKE) during the pollution episode at different heights (the shaded area indicate the surface PM_{2.5} concentration).

December 29 to 1600 LST December 30. The PM_{2.5} concentration in Tianjin remained at a high level of approximately 240 $\mu\text{g m}^{-3}$. During this period, a weak wind prevailed near ground level and the relative humidity remained greater than 70%. In addition, a temperature inversion layer was observed at altitudes between 140 and 250 m on December 30 that greatly restrained the vertical diffusion of air pollutants. (4) During the dissipation stage (Stage 4), a strong northwesterly wind (approximately 4–6 m s^{-1}) began in the afternoon of December 30 and led to the substantial improvement of pollutant diffusion conditions. The relative humidity decreased rapidly to below 50% and the PM_{2.5} concentration dropped sharply to 40 $\mu\text{g m}^{-3}$, indicating the end of this pollution episode.

3.2. Impacts of vertical turbulent diffusion on this pollution episode

Changes in the PM_{2.5} concentration were closely associated with the impacts of the turbulence characteristics within the PBL. Fig. 6 shows the temporal variations of turbulent kinetic energy (TKE) during the investigation period, along with the corresponding surface PM_{2.5} mass concentrations. The TKE variations were quite similar at the three different heights. Furthermore, a clear negative relationship could be observed between the PM_{2.5} concentrations and turbulence intensities. Before the occurrence of the pollution episode (i.e., in the primary stage), turbulent exchange is quite active (up to $4.8 \text{ m}^2 \text{ s}^{-2}$ at 200 m) which keeps the PM_{2.5} concentration at a quite low level. Turbulence in the PBL became weaker during the rapid formation and maintenance stages of the haze episode with the TKE decreasing to $0.1 \text{ m}^2 \text{ s}^{-2}$. However, in the early morning of Dec 28, due to the cooling effect of the longwave radiation of water droplets (RH reached 95%, see Fig. 5b), turbulence strengthened (the TKE increased to $0.8 \text{ m}^2 \text{ s}^{-2}$) and the PM_{2.5} concentration decreased simultaneously (see Fig. 6). The stationary phase of the turbulent motion continued until the noon on Dec 29, when the TKE at 40 m increased to $2.0 \text{ m}^2 \text{ s}^{-2}$ due to solar heating at ground level and leveled off thereafter. As a result, the PM_{2.5} concentration exhibited a temporary dip and then returned to a high level. Starting on the afternoon of December 30 (the dissipation stage), there was an evident increase in the TKE (up to $11.6 \text{ m}^2 \text{ s}^{-2}$ at 200 m), which indicated that the turbulent diffusion capacity began to strengthen with pollution dissipation. The tight corresponding relationship between the TKE and PM_{2.5} levels indicated the key role of turbulent motions in the vertical mixing and distribution of chemical species.

3.3. Model evaluation

3.3.1. Evaluation of surface meteorological variables and PM_{2.5} concentration

Fig. 7 presents the time series of observed and modeled hourly 2-m temperature (T2), 2-m relative humidity (RH2), 10-m wind speed (WS10) and surface PM_{2.5} for all cases from 0000 LST 27 December to 0300 LST 31 December 2017 in Tianjin. All five PBL schemes could satisfactorily capture the diurnal variations of surface meteorological

variables. For the case of T2, there is a general underestimation of the diurnal temperature range, in comparison with the observations, namely, underestimation of the daily maximum temperature (by up to 5 °C) and overestimation of the nighttime minimum temperature (by up to 8 °C). The observed RH2 varies within the range of 19% to 94% during the study period. An obvious overestimation of the modeled air humidity (by ~22%) is noticed from Dec 28 to Dec 30. The modeled WS10 values are higher by 1–6 m s^{-1} than the observations. An overestimation of winds in the WRF model has been documented in several works (Madala et al., 2015; Sathyanadh et al., 2017), mainly due to the inaccurate description of surface roughness and induced turbulence motion in the surface layer. For the surface PM_{2.5}, the observed PM_{2.5} concentration was high during the nighttime and low during the daytime, which was reasonably consistent with the modeled values. Throughout the study period, the observed mean and peak values of the surface PM_{2.5} concentration were 241 and 129 $\mu\text{g m}^{-3}$, respectively. The modeled PM_{2.5} concentrations generally captured the diurnal variation patterns but exhibited large positive deviations during the nighttime. Table 3 presents the statistics for the simulated meteorological and air quality variables of different PBL schemes. As shown in Table 3, the MYJ PBL scheme generally exhibited the best performance with relatively smaller MB, MAB, RMSE values and larger R and IOA values for both meteorological and air quality parameters at the surface.

Furthermore, to evaluate the model performance in reproducing the evolution tendency of PBLH, the modeled PBLHs were validated against the ceilometer observations collected during this episode (Table 4). In general, the PBLHs from all PBL schemes showed similar behaviors with clear underestimations (MB up to −324.3 m), in comparison with the observations. PBLH determines the available volume for the dispersion of air pollutants released at the surface, hence the underestimation of PBLH may be the primary reason for the positive deviations in the simulated PM_{2.5} concentrations (see Fig. 7d). Likewise, the MYJ scheme shows the best performance in reproducing the diurnal variations of PBLH with the smallest MAB.

3.3.2. Comparisons of the vertical structures of PBL physical and chemical properties simulated with different PBL schemes against the observations

The vertical profiles of the physical (air temperature, relative humidity and wind speed) and chemical (PM_{2.5} concentration) properties of the urban boundary layer derived from simulations are also compared with tethered balloon-based sounding observations. To fully test the accuracy of vertical structure of atmospheric pollution simulated by different PBL schemes, comparisons and validations are performed separately for each pollution stage (stages 1–4 as mentioned above). Fig. 8 shows the observed and simulated vertical profiles of air temperature at four representative hours on behalf of the primary stage, the rapid formation stage, the maintenance stage and the dissipation stage, respectively. In the clean stage (Fig. 8a), simulations using all five parameterizations predict higher temperatures than observations in the lower to medium levels (0–700 m), implying an error source that was common to all the model runs. A strong elevated inversion layer (at altitudes above 600 m with an intensity of 3.8 °C/100 m) could be observed during the rapid formation and maintenance stages (Fig. 8b and c). All the model runs capture the occurrence of the elevated temperature inversion (TI), whereas none of them could properly reproduce the height or the intensity of the TI. For example, the YSU runs underestimate the height of the inversion layer at 0200 LST on Dec 29 and the ACM2 runs predict much weaker intensity of the temperature inversion at 0800 LST on Dec 29. The elevated TI acts as a cap that prevents the vertical mixing between polluted air below and the relatively cleaner air above. Underestimation of the height of TI layer would limit the dispersion of air pollutants, hence lead to an overestimation of pollutant concentrations. No TI layer was observed during the dissipation stage (Fig. 8d), which suggests amelioration of the vertical diffusion conditions. All five PBL

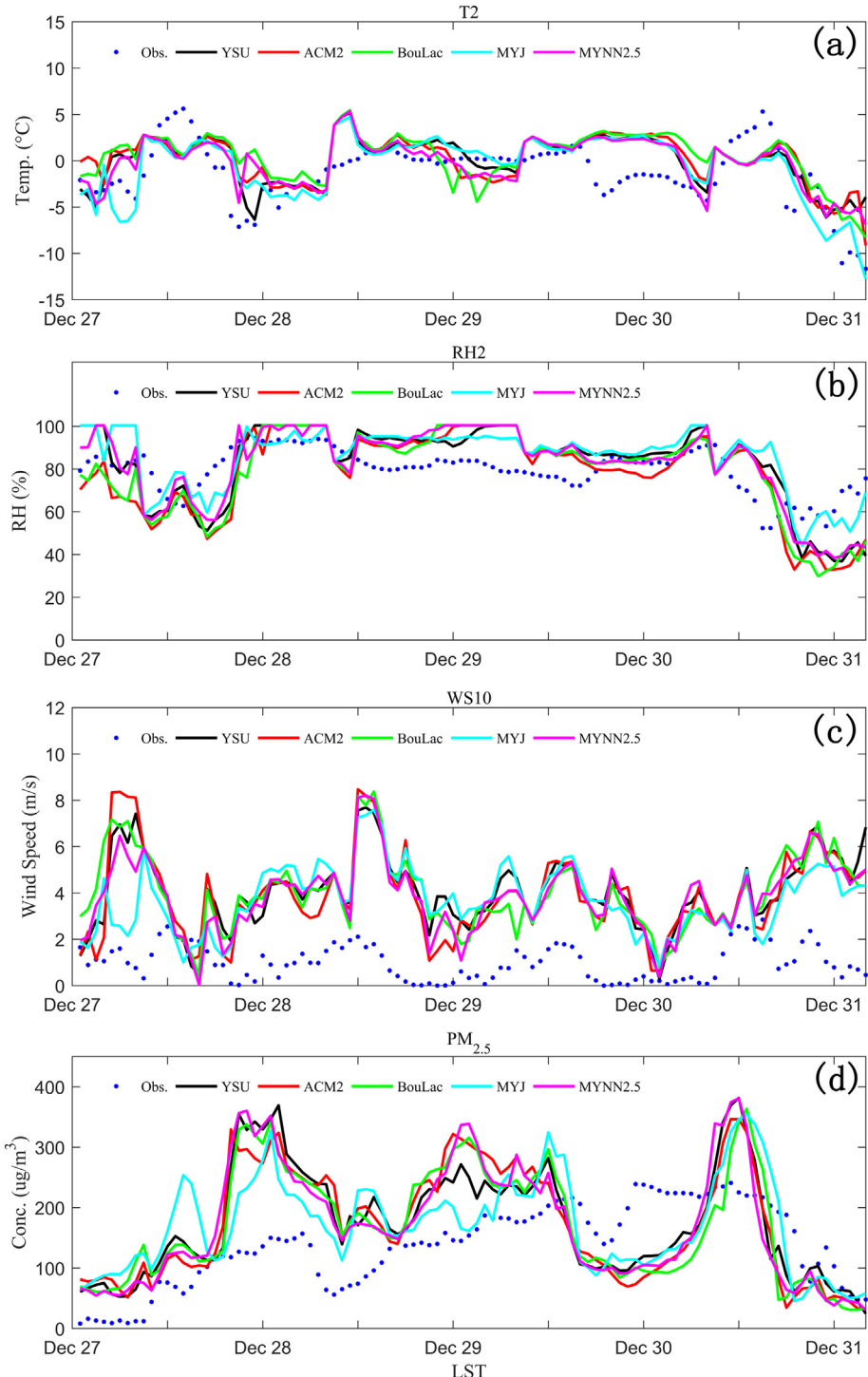


Fig. 7. Comparison of T2 (a), RH2 (b), WS10 (c) and PM_{2.5} concentrations (d) time series modeled by WRF-Chem with different PBL schemes against observations during the experimental period in Tianjin.

schemes fail to capture the damage of the inversion layer, which was likely caused by an underestimation of the vertical mixing within the PBL.

The RH profiles simulated by the five experiments show larger differences than the temperature profiles, as is shown in Fig. 9. All the model runs generally underestimate the ambient RH during the clean stage, with the MYJ run exhibiting the least bias, especially below 250 m (see Fig. 9a). In the rapid formation and maintenance stages, the observed RHs rise remarkably (to approximately 87%) below 600 m. Under these circumstances, the hygroscopic growth of airborne

particles would play important roles, and hence may be a primary cause of the formation and maintenance of the haze pollution. All the PBL schemes tend to predict much more water vapor (even to saturation) than the observations in the lower atmosphere. In addition, there is drastic reductions in the observed RH profiles (to 40%) between 600 and 800 m. All five simulations capture the abrupt changes in RH profiles above 200 m or higher. Nonetheless, errors still exist in the thickness of the high-humidity layer (RH > 80%), with the MYJ scheme giving the best results compared to the observations. In the dissipation stage, the observed surface RHs decreased noticeably (to 56%), leading

Table 3

Statistical analysis of modeled 2-m temperature (°C), relative humidity (%), 10-m wind speed (m s^{-1}) and surface $\text{PM}_{2.5}$ concentration ($\mu\text{g m}^{-3}$) for different PBL schemes against surface observations during the experimental period. (The shaded cells represent the best performance in each row.)

		YSU	ACM2	BouLac	MYJ	MYNN
T2	MB	1.7	1.8	2.1	1.0	1.5
	MAB	3.3	3.5	3.6	3.0	3.1
	RMSE	4.2	4.3	4.5	3.8	4.0
	R	0.56	0.53	0.52	0.62	0.60
	IOA	0.63	0.63	0.63	0.75	0.68
RH2	MB	-0.8	-6.4	-4.1	4.3	-1.2
	MAB	15.8	16.6	14.9	14.0	14.6
	RMSE	19.5	21.7	18.7	16.9	18.0
	R	0.51	0.48	0.56	0.52	0.56
	IOA	0.70	0.67	0.73	0.71	0.73
WS10	MB	3.4	3.4	3.2	3.0	3.2
	MAB	3.4	3.4	3.3	3.1	3.3
	RMSE	3.8	3.9	3.7	3.5	3.7
	R	0.45	0.46	0.50	0.46	0.50
	IOA	0.36	0.35	0.37	0.38	0.37
PM _{2.5}	MB	40.2	37.7	36.8	35.7	37.7
	MAB	80.3	85.8	85.9	72.1	84.5
	RMSE	94.7	99.4	99.2	83.8	99.0
	R	0.40	0.33	0.31	0.42	0.38
	IOA	0.57	0.54	0.52	0.62	0.56

to suppressed hygroscopic growth of aerosols. A layer of a somewhat constant RH (~62%) is noted between 100 and 500 m, and the ambient RH began to decrease above a height of 500 m. The simulated RH profiles reproduce this drying event with a reduction in RH of up to 25% at the surface as well as at higher levels, but all of the schemes tend to produce large low-level RHs (>75%) and fail to predict the constant-RH layer with an altitude in the range of 100–500 m that was observed in the dissipation stage of this haze episode.

The observed and simulated vertical wind profiles in the different stages of this haze episode are presented in Fig. 10. In the primary stage, the wind speed from all schemes exhibit similar behaviors with clear overestimations compared with the observations throughout the PBL. The observed vertical wind speed distributions remains at relatively low levels (no larger than 5 m s^{-1} below 800 m) during the rapid formation and maintenance stages of the haze episode. The modeled winds are generally higher by $2\text{--}3 \text{ m s}^{-1}$ than the observations in the near-surface layer, whereas underestimations to some extent are observed in the layer above. In the dissipation stage of this episode, all of the model runs clearly overestimated the wind speed gradients, i.e., the model tends to predict weaker winds at the surface, while at the layer above, the modeled winds are typically overestimated. The discrepancies in the calculations of the wind speed gradients against the

observations can be associated with the inaccurate representations of the eddy exchange coefficient within the PBL.

Tables 5 and 6 summarize the model performance metrics of WRF-Chem against the vertical sounding measurements of meteorological parameters for different stages of the pollution episode. To provide a concise and intuitive assessment of different PBL schemes, we further classify the primary stage and dissipation stage into the clean period (Table 5), and the formation stage and maintenance stage into the polluted period (Table 6). In general, the statistical results show that the MYJ scheme could predict more realistic temperature and humidity profiles during the polluted period, for the MYJ run gives the top two performances for most of the statistical metrics (see Table 6). For the wind profiles, all the PBL schemes show similar behaviors, with normalized MB larger than 45% (not shown in the table). The discrepancies in the wind profiles between the model predictions and observations suggest that a high level of uncertainty still exists in the parameterization of the eddy exchange coefficient within the PBL. For the clean period, the MYJ run shows poor agreement with the sounding profiles and the vertical distribution of meteorological variables is better simulated by the ACM2 scheme. These findings reflect the weakness of the MYJ scheme in correctly capturing the vertical turbulent mixing under unstable stratifications, which is the typical meteorological condition for the dissipation stage of pollution episodes. Some relevant studies have also concluded that nonlocal PBL schemes generally performs better than local PBL schemes in predicting vertical meteorological profiles when the atmospheric stability is weaker (Hu et al., 2010; Banks et al., 2016). Moreover, Jahn et al. (2017) indicated that there is much room for improvement in wind forecasts that use mesoscale models, especially at the near-surface level, and such improvements inevitably require modifications to the PBL parameterization schemes.

Statistical indicators are also calculated to evaluate the abilities of the five PBL schemes in simulating the vertical $\text{PM}_{2.5}$ distributions (Table 7) for both the clean and polluted periods. The results show that the MYJ scheme gives the best performance for the polluted period, with the smallest (or 2nd smallest) MAB and RMSE values and highest IOA and FAC2 values. However, for the clean period, adoption of the MYJ PBL parameterization shows poor agreement with the sounding observations while the ACM2 scheme generally performs better, which is in accordance with the assessment results of the meteorological factors. These findings prove again the key role of the meteorological fields in modeling atmospheric chemical processes. Banks and Baldasano (2016) also found that ACM2 generally produces better results than the other PBL schemes (YSU, MYJ and BouLac) for air quality simulations conducted for the northeastern Iberian Peninsula, with a modeled period dominated by a regional recirculation synoptic flow regime. The results of these studies suggest that there is not an optimal PBL scheme for all cases but that the performance varies depending on the atmospheric conditions. The poor and diverse performance of the vertical $\text{PM}_{2.5}$ profiles simulated by the different PBL schemes highlights the need for further model improvements to estimate the vertical distributions of chemical species in a more realistic way, especially during severe haze episodes.

3.3.3. Comparisons of the vertical structures of the PBL turbulence properties simulated with MYJ against the observations

Turbulent motion is the natural property of atmospheric dynamics within the PBL. Different parameterizations of turbulent exchange processes can affect the predicted meteorology and chemistry in the lower atmosphere to a large extent. As mentioned above, clear discrepancies are found between the model predictions and observations of the wind and $\text{PM}_{2.5}$ vertical profiles, especially during the primary and dissipation stages. Uncertainties in the turbulent exchange coefficient among different PBL parameterizations are considered to be one of the major sources of model discrepancies. Nonetheless, measurements of the vertical structure of PBL turbulence properties are so scarce that few studies have used turbulence information to evaluate PBL schemes

Table 4

Statistical analysis of modeled PBLH (m) for different PBL schemes against ceilometer observations during the experimental period. (The shaded cells represent the best performance in each row.)

		YSU	ACM2	BouLac	MYJ	MYNN
PBLH	MB	-324.3	-263.5	-271.8	-271.7	-128.5
	MAB	365.6	372.2	388.0	351.6	373.5
	RMSE	515.7	525.9	550.9	489.6	508.3
	IOA	0.42	0.41	0.40	0.46	0.36

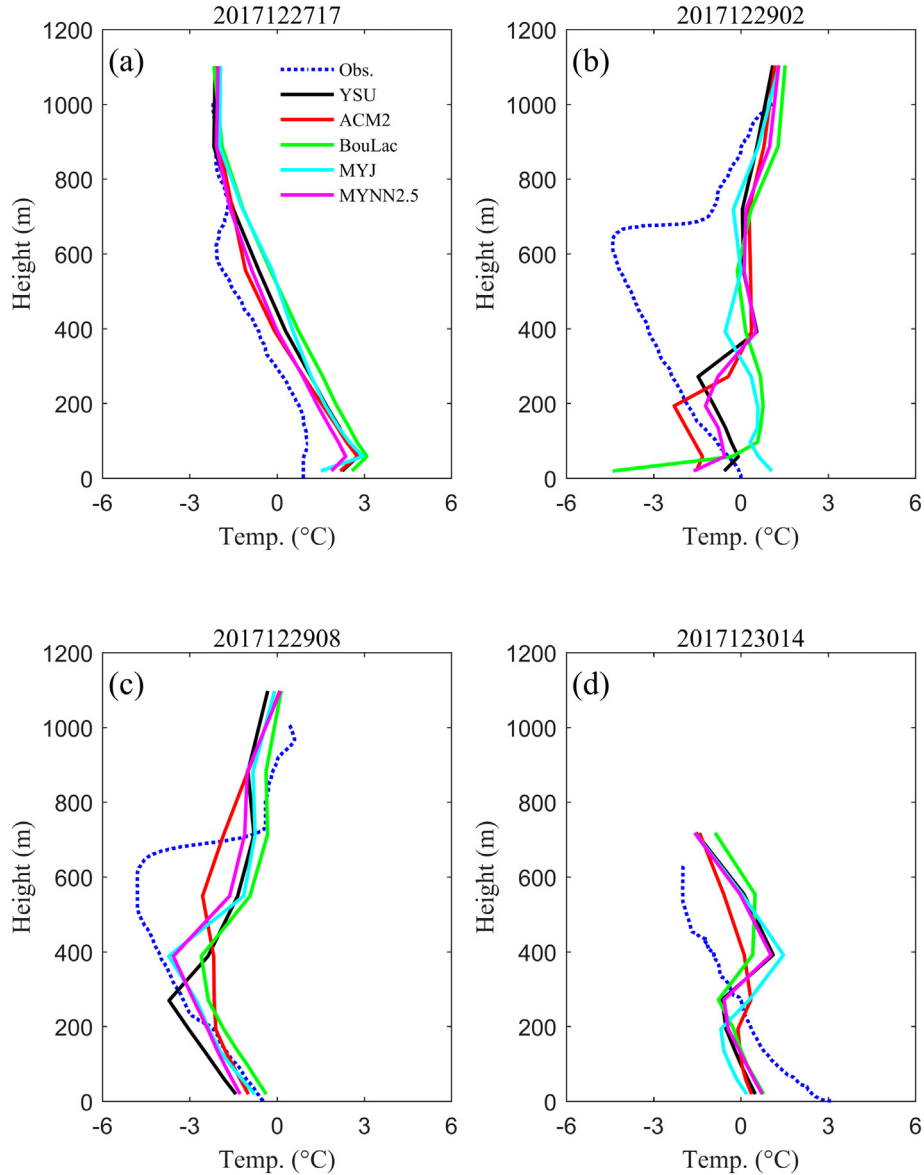


Fig. 8. Comparison of observed vs. modeled air temperature vertical profiles with different WRF PBL schemes during the (a) clean stage, (b) rapid formation stage, (c) maintenance stage and (d) dissipation stage.

(Munoz-Esparza and Sharman, 2018). To fill the knowledge gap so as to accurately represent the vertical PBL structure for the case of pollution episodes, the vertical distributions of the turbulent exchange coefficient are discussed in the present study, which are derived from the sounding temperature and wind profiles following the algorithm proposed by Blackadar (1962) and Estoque and Bhumralkar (1970).

The turbulent exchange coefficient (K_m) is defined as:

For neutral conditions,

$$K_m = \varepsilon^{1/3} l^{4/3} \quad (11)$$

where ε is the turbulent dissipation rate per unit mass, l is the characteristic scale of turbulent eddies, namely, the mixing length scale:

$$\varepsilon = K_m \left[\left(\frac{du}{dz} \right)^2 + \left(\frac{dv}{dz} \right)^2 \right] \quad (12)$$

$$l = \frac{kz}{1 + \frac{kz}{\lambda}} \quad (13)$$

$$\lambda = 2.7 \times \frac{10^{-5} v_g}{f} \quad (14)$$

where k is the von Karman constant ($= 0.4$), v_g is the geostrophic wind speed and f is the Coriolis parameter.

For unstable conditions,

$$K_m = l^2 \frac{d\bar{v}}{dz} (1 - a_0 s) \quad (15)$$

For stable conditions,

$$K_m = l^2 \frac{d\bar{v}}{dz} (1 + a_0 s)^{-1} \quad (16)$$

$$s = \frac{(gl)^{1/2}}{\theta} \left(\frac{\partial \theta}{\partial z} / \frac{\partial u}{\partial z} \right) \quad (17)$$

$$\frac{d\bar{v}}{dz} = \left[\left(\frac{du}{dz} \right)^2 + \left(\frac{dv}{dz} \right)^2 \right]^{1/2} \quad (18)$$

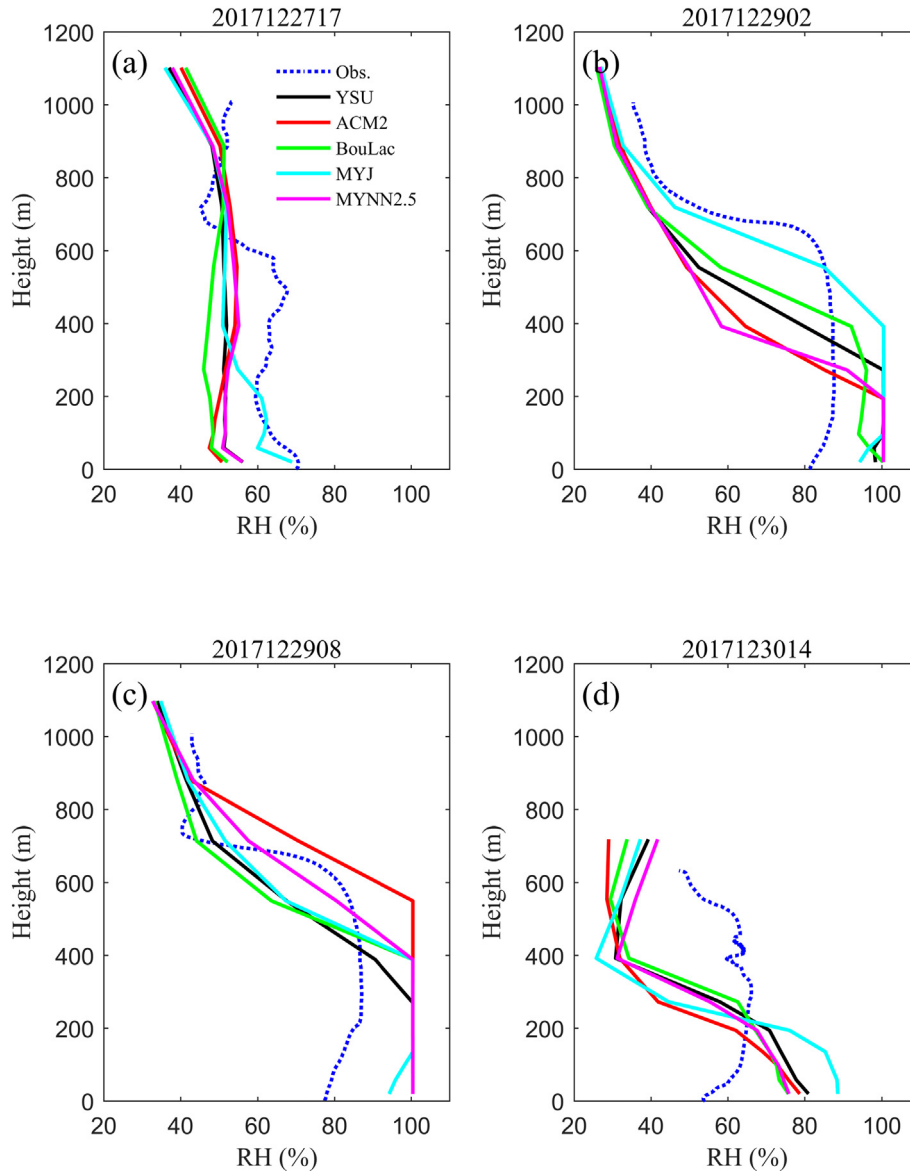


Fig. 9. Same as Fig. 8, but for relative humidity.

where a_0 is an empirical constant following Estoque and Bhumralkar (1970), θ is the potential temperature and u and v are the horizontal wind components.

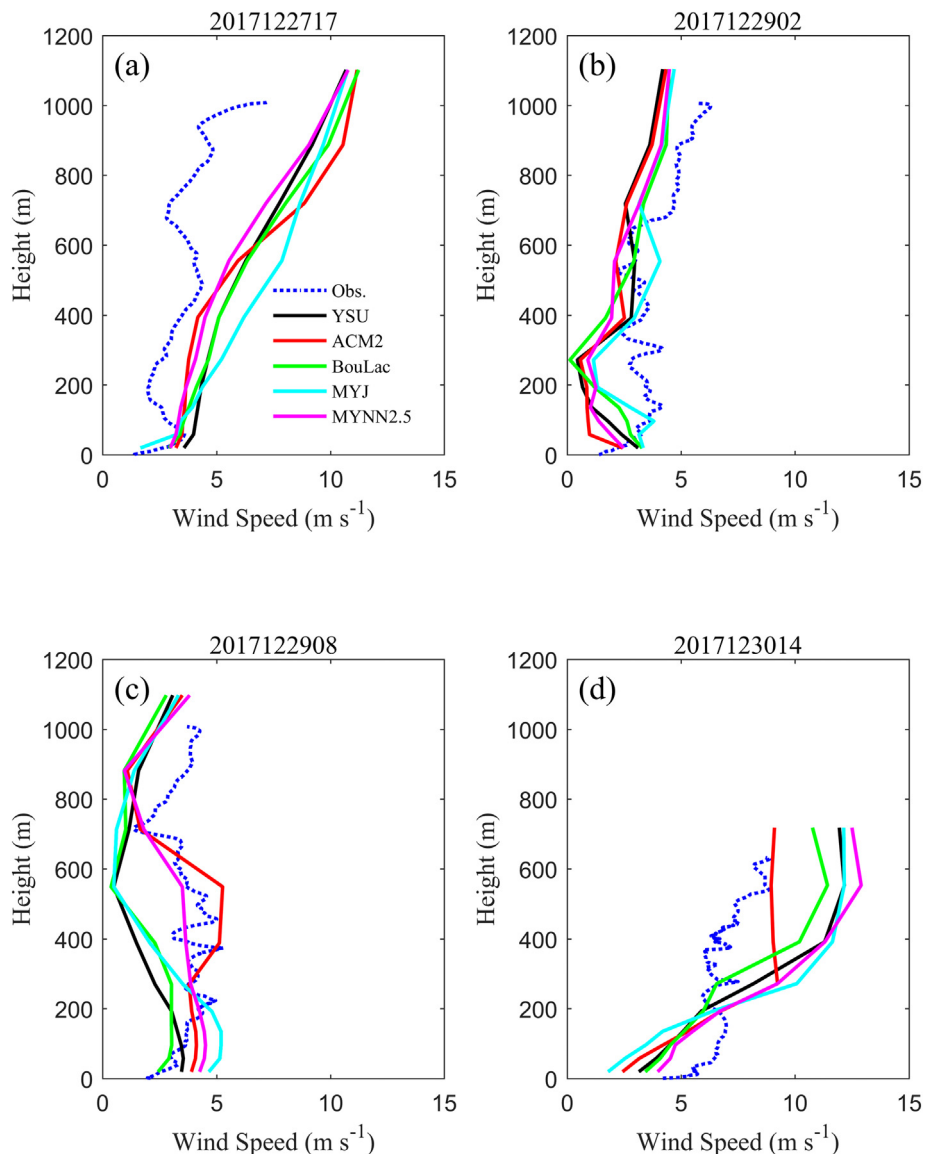
Fig. 11 exhibits the simulated turbulent exchange coefficient (K_m) produced by the MYJ scheme against the corresponding observation results derived from the above Eqs. (11)–(18). As seen in Fig. 11, the MYJ scheme produces comparable K_m values compared to the observations during the rapid formation and maintenance stages with slight underestimations. During the primary and dissipation stages, the observed K_m profiles show an evident enhancement especially at heights from approximately 200–400 m. However, for the modeled profiles, minor differences could be distinguished between the different stages of the haze episode, which lead to large discrepancies compared to observations. These results reflect the failure of MYJ to accurately distinguish the intensity of turbulent mixing between different stages of haze episodes. This deficiency of the MYJ scheme, which is caused by the inherent uncertainties in PBL parameterization, are expected to have induced considerable errors in the predicted vertical structure of wind fields and $PM_{2.5}$ concentrations. This finding agrees with Wang et al. (2018) who found that PBL parameterizations require further improvements in the

representations of turbulent diffusion processes for accurate predictions of severe haze events.

3.4. Sensitivity analysis of MYJ with different turbulence parameters

As mentioned above, MYJ is generally found to be statistically superior to other PBL schemes for the simulation of winter haze events. However, MYJ performs relatively poorly in simulations of vertical wind and K_m profiles during the primary and dissipation stages, which reveals the insufficient ability of MYJ in distinguishing the intensity of turbulent mixing between different stages of haze episodes. Further improvement of PBL parameterization is indispensable for accurate prediction of haze episode, which would be discussed in this section.

In the present study, we would investigate the impact of Pr on the performance of the WRF-Chem model by using numerical experiments as described in the methodology section. Fig. 12 shows the vertical profiles of the meteorological variables and $PM_{2.5}$ concentrations as simulated by the MYJ PBL scheme due to different Pr values (i.e., MYJ0.5–2.0) for the winter haze case. The observation data obtained from radiosonde soundings are employed to evaluate the modeled temperature, humidity and wind speed profiles for different sensitivity cases. As

**Fig. 10.** Same as Fig. 8, but for wind speed.**Table 5**

Statistical analysis of modeled temperature ($^{\circ}\text{C}$), relative humidity (%) and wind speed (m s^{-1}) for different PBL schemes against balloon sounding measurements during the clean period. (The shaded cells represent the best performance in each row.)

Clean period					
	YSU	ACM2	BouLac	MYJ	MYNN
Temperatur ($^{\circ}\text{C}$)	MB	0.4	0.5	0.8	0.5
	MAB	1.8	1.5	1.7	1.9
	RMSE	1.9	1.8	1.8	2.1
	IOA	0.53	0.63	0.50	0.48
RH (%)	MB	-8.1	-12.3	-9.6	-3.9
	MAB	14.8	17.1	15.2	12.2
	RMSE	17.4	20.1	18.5	15.5
	IOA	0.68	0.58	0.65	0.74
Wind Speed (m s^{-1})	MB	1.0	0.9	1.0	1.4
	MAB	1.8	1.7	1.8	2.1
	RMSE	2.4	2.3	2.3	2.7
	IOA	0.70	0.69	0.71	0.66

Table 6

Statistical analysis of modeled temperature ($^{\circ}\text{C}$), relative humidity (%) and wind speed (m s^{-1}) for different PBL schemes against balloon sounding measurements during the polluted period. (The shaded cells represent the best performance in each row.)

	Polluted period				
	YSU	ACM2	BouLac	MYJ	MYNN
Temperatur ($^{\circ}\text{C}$)	MB	0.4	0.5	0.8	0.6
	MAB	1.5	1.5	1.6	1.3
	RMSE	1.9	1.9	2.0	1.7
	IOA	0.59	0.56	0.50	0.63
RH (%)	MB	8.9	8.2	7.5	10.1
	MAB	17.1	16.8	15.1	16.7 ^{2nd}
	RMSE	18.6	18.5	17.3	18.0 ^{2nd}
	IOA	0.75	0.75	0.77	0.78
Wind Speed (m s^{-1})	MB	0.9	1.0	1.0	1.6
	MAB	1.7	1.6	1.7	2.1
	RMSE	2.1	2.1	2.1	2.6
	IOA	0.59	0.59	0.53	0.52

^{2nd}The prediction skill of the MYJ run ranked 2nd in all five simulation experiments for the individual index.

Table 7

Statistical analysis of $\text{PM}_{2.5}$ concentration ($\mu\text{g m}^{-3}$) for different PBL schemes against balloon sounding measurements during the clean and the polluted period. (The shaded cells represent the best performance in each row.)

Clean period					
	YSU	ACM2	BouLac	MYJ	
MB	0.5	3.2	14.4	-0.1	3.6
MAB	55.9	54.1	60.9	64.7	54.8
RMSE	77.2	72.6	81.2	87.4	76.0
IOA	0.55	0.57	0.51	0.46	0.52
FAC2	0.73	0.78	0.74	0.70	0.68
Polluted period					
	YSU	ACM2	BouLac	MYJ	
MB	2.4	11.76	5.4	-11.5	10.6
MAB	48.7	51.0	52.6	49.4 ^{2nd}	54.6
RMSE	63.7	65.6	65.6	61.5	73.0
IOA	0.66	0.66	0.63	0.69	0.66
FAC2	0.85	0.84	0.82	0.86	0.81

^{2nd}The prediction skill of the MYJ run ranked 2nd in all five simulation experiments for the individual index.

seen in Fig. 12, all experiments overestimated the intensity of the temperature inversions near the surface and failed to reproduce the inversion layer at altitudes near 600 m, which may be due to an inadequate representation of the PBL parameters that account for the turbulent exchange processes. The modeled RHs generally capture the vertical distribution patterns of the observations except for a slight overestimation near the surface. Wind speeds are generally overestimated throughout the PBL, especially at the lower levels. In the comparisons of different experiments, the modeled profiles vary considerably with

the different Pr values, which indicates that the vertical distribution of the meteorological fields are directly associated with the vertical turbulent exchange coefficients, especially in the lower levels. Turbulence parameters also play a crucial role in the distribution of air pollutant concentrations by affecting the vertical mixing processes. As shown in Fig. 12(d), the WRF-Chem simulations of the $\text{PM}_{2.5}$ concentrations are highly sensitive to the selection of Pr values, and this sensitivity is more prominent in the lower atmosphere.

Table 8 shows the statistical verification results for the vertical distributions of temperature, water vapor, wind speed and $\text{PM}_{2.5}$ concentrations with different Pr values during the air pollution episode. The results indicate that a Pr value of 2.0 can lead to an overall improvement in the simulations of the vertical profiles of temperature, wind speed and $\text{PM}_{2.5}$ concentrations.

4. Conclusions

To explore the impact of PBL parameterizations on the simulations of a winter haze episode in a coastal urban environment of the BTH region, China, a series of numerical experiments using the WRF-Chem model were conducted in this study. We tested the sensitivity of model performance to five different PBL schemes (YSU, ACM2, MYJ, MYNN2.5 and BouLac) in comparison with observations. Through validation against the hourly variation trends of the near surface observations, the MYJ scheme generally produced the best performance for both the meteorological and air quality factors among all five PBL schemes. Additionally, to present a direct and more complete assessment, the model simulations are further compared with the observation data in the vertical

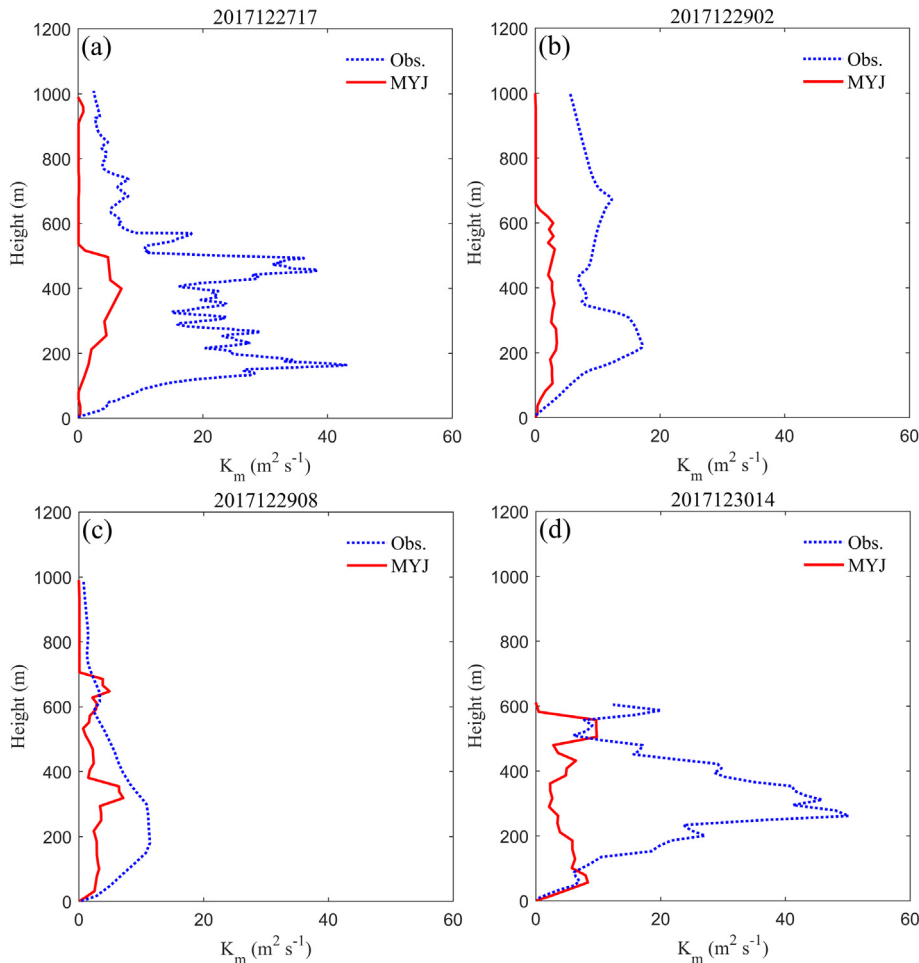


Fig. 11. Comparison of observed vs. MYJ modeled vertical profiles of turbulent exchange coefficient (K_m) during the (a) primary stage, (b) rapid formation stage, (c) maintenance stage and (d) dissipation stage.

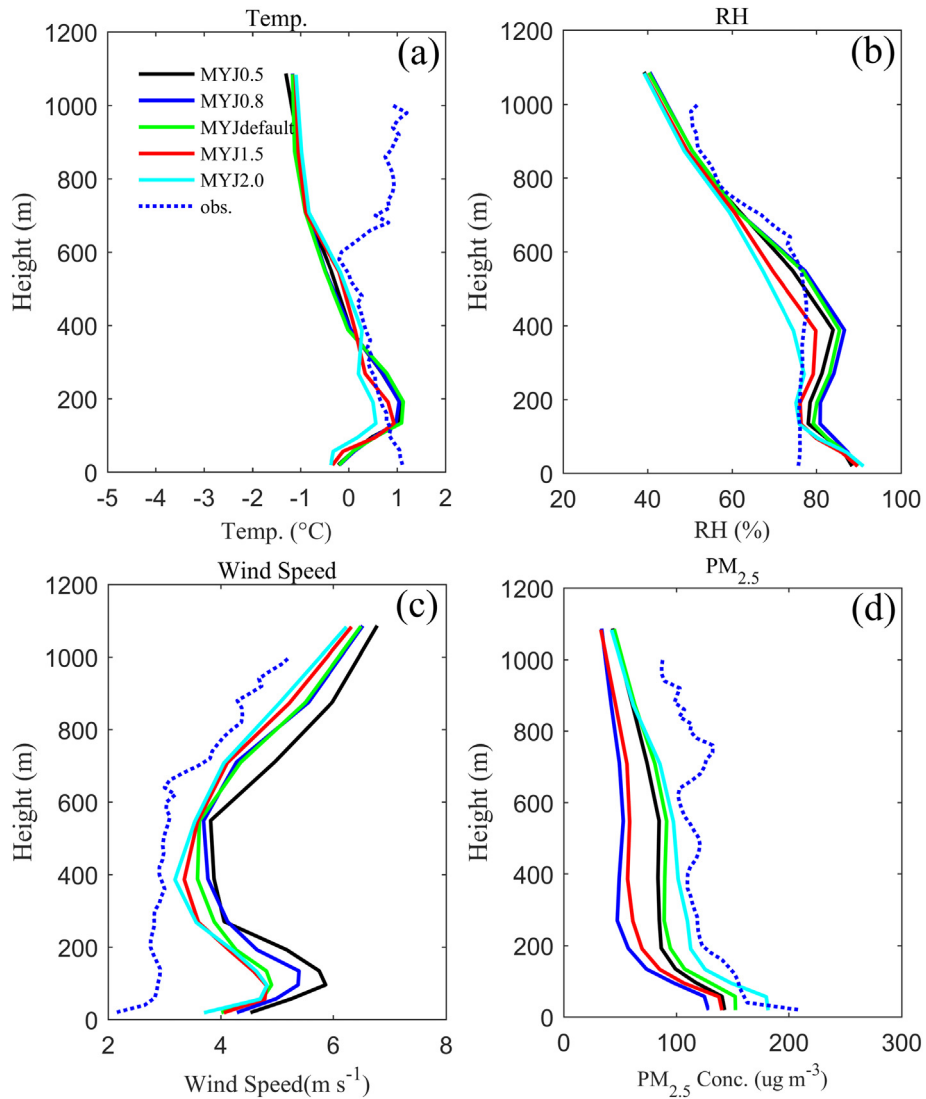


Fig. 12. Comparison of observed vs. MYJ modeled vertical profiles of (a) temperature, (b) relative humidity, (c) wind speed and (d) PM_{2.5} concentrations with different Pr values averaged during the haze episode.

profiles of both the meteorological and air quality quantities derived from a tethered balloon platform. The results of the direct assessments suggest that MYJ generally outperform the other schemes in predicting the vertical profiles of temperature, humidity and PM_{2.5} concentrations during the formation and maintenance stages of the pollution episode. However, during the relatively clean period, the MYJ run shows poor agreement with the sounding profiles, while the vertical trends of the variables are better simulated by the ACM2 scheme, reflecting the weakness of MYJ for correctly capturing vertical turbulent mixing under unstable stratifications. With respect to the wind profiles, all the PBL schemes perform similarly with the normalized MB exceeding 45%. The discrepancies in the wind profiles between the model predictions and observations can be attributed to some inherent deficiencies caused by the high degree of uncertainty that still exists in the parameterizations of the eddy exchange coefficient within the PBL. To confirm this diagnosis, the vertical distribution of turbulent exchange coefficient is discussed in the present study and compared against MYJ simulations. The comparison analyses reveal the insufficient ability of MYJ in distinguishing the turbulent diffusion strengths between different stages of the haze episode, which may be a major source of model bias and requires further improvement for accurate predictions of severe haze events.

Overall, MYJ is found to be statistically superior to the other schemes for the simulation of winter haze events but still needs further improvements to reduce model errors. A series of parametric sensitivity experiments are conducted with different Pr values, and the analysis results indicate that the model predictions, both of meteorological and air quality variables, are quite sensitive to the choice of Pr value. The default parameters used in the original MYJ formulation ($Pr = 1.0$) are not the best for this specific case; instead, a Pr value of 2.0 shows the greatest agreement with observations for both the vertical profiles and horizontal distributions. Accordingly, we conclude that the new set of MYJ closure parameters (corresponding to the Pr value of 2.0) can lead to an overall improvement in the representation of turbulent diffusion in the MYJ PBL scheme and hence should be adopted for accurate predictions of winter haze events in China's BTB region.

Although we have directly and comprehensively examined the applicability of different PBL schemes and have proposed a new set of closure parameters that can result in marked forecast improvements for winter haze episodes in the BTB region of China, there are still limitations in this study. It should be noted that the haze cases employed for sensitivity analyses in this study are limited, and there is no single run, either for different PBL schemes or for different parameter values, that shows the overall best performance for forecasts of all variables for different stages of the haze episode. In fact, in the latest published

Table 8

Statistical analysis of air temperature, relative humidity, wind speed and PM_{2.5} concentration for different experiments (MYJ0.5–MYJ2.0) against balloon sounding measurements during the haze episode. (The shaded cells represent the best performance in each row.)

Air temperature					
	MYJ0.5	MYJ0.8	MYJdefault	MYJ1.5	MYJ2.0
MB	0.5	0.5	0.6	0.4	0.4
MAB	1.4	1.3	1.3	1.3	1.3
RMSE	1.6	1.6	1.6	1.6	1.6
IOA	0.65	0.64	0.64	0.64	0.62
Relative humidity					
MB	3.4	3.5	2.7	0.0	-1.2
MAB	14.8	14.5	15.0	16.6	17.1
RMSE	17.4	17.2	17.5	19.3	19.8
IOA	0.75	0.75	0.74	0.69	0.68
Wind speed					
MB	1.7	1.6	1.5	1.3	1.1
MAB	2.3	2.2	2.1	1.9	1.9
RMSE	3.0	2.7	2.7	2.4	2.3
IOA	0.62	0.66	0.68	0.71	0.72
Concentration of PM _{2.5}					
MB	-40.5	-63.0	-33.8	-55.2	-23.6
MAB	61.0	74.3	59.6	70.3	56.4
RMSE	79.6	92.8	77.7	88.0	76.0
IOA	0.54	0.50	0.53	0.52	0.55
FAC2	0.72	0.49	0.77	0.57	0.76

review by Li (2019), the author suggested that Pr would decrease as the atmosphere becomes more stable; however, studies examining the role of Pr in weather and climate models are surprisingly sparse. This is quite in line with the conclusion obtained in our study which indicates that a larger Pr (=2.0), rather than the default value in the MYJ formulation (=1.0), is more applicable for model simulations under stable atmospheric conditions. Hence, as a reasonable inference, it may be more appropriate that the PBL parameter values should be specifically assigned depending on the PBL structures under different meteorological and geophysical circumstances. To address this issue, more cases are needed in the future work, including different test areas under different synoptic conditions, in order to acquire more universal conclusions.

CRediT authorship contribution statement

Jianbo Yang: Conceptualization, Methodology, Writing - original draft. **Yingxiao Tang:** Investigation. **Suqin Han:** Data curation, Supervision, Writing - review & editing, Funding acquisition. **Jingle Liu:** Resources. **Xu Yang:** Formal analysis. **Jian Hao:** Validation.

Declaration of competing interest

The authors declare that they have no known competing financial interests or personal relationships that could have appeared to influence the work reported in this paper.

Acknowledgements

This work was funded by the National Natural Science Foundation of China (41771242), the Natural Science Foundation of Tianjin (18JCYBJC23100), and the Scientific research project of Tianjin Meteorological Bureau (202130zdxm02).

References

- An, J.L., Cheng, X.J., Qu, Y., Chen, Y., 2007. Influence of vertical eddy diffusivity parameterization on daily and monthly mean concentrations of O₃ and NO_x. *Adv. Atmos. Sci.* 24 (4), 573–580.
- Avolio, E., Federico, S., Miglietta, M.M., Feudo, T.L., Calidonna, C.R., Sempreviva, A.M., 2017. Sensitivity analysis of WRF model PBL schemes in simulating boundary-layer variables in southern Italy: an experimental campaign. *Atmos. Res.* 192, 58–71.
- Banks, R.F., Baldasano, J.M., 2016. Impact of WRF model PBL schemes on air quality simulations over Catalonia, Spain. *Sci. Total Environ.* 572, 98–113.
- Banks, R.F., Tiana-Alsina, J., Baldasano, J.M., Rocadenbosch, F., Papayannis, A., Solomos, S., Tzanis, C.G., 2016. Sensitivity of boundary-layer variables to PBL schemes in the WRF model based on surface meteorological observations, lidar, and radiosondes during the HygrA-CD campaign. *Atmos. Res.* 176–177, 185–201.
- Blackadar, A.K., 1962. The vertical distribution of wind and turbulent exchange in a neutral atmosphere. *J. Geophys. Res.* 67, 3095–3102.
- Bougeault, P., Lacarrère, P., 1989. Parameterization of orography-induced turbulence in a meso-beta scale model. *Mon. Weather Rev.* 117, 1872–1890.
- Chaouch, N., Temimi, M., Weston, M., Ghedira, H., 2017. Sensitivity of the meteorological model WRF-ARW to planetary boundary layer schemes during fog conditions in a coastal arid region. *Atmos. Res.* 187, 106–127.
- Chen, D.S., Xie, X., Zhou, Y., Liang, J.L., Xu, T.T., Yang, N., Zhao, Y.H., Liu, X.X., 2017. Performance evaluation of the WRF-Chem model with different physical parameterization schemes during an extremely high PM_{2.5} pollution episode in Beijing. *Aerosol Air Qual. Res.* 17, 262–277.
- Cohen, A.E., Cavallo, S.M., Coniglio, M.C., Brooks, H.E., 2015. A review of planetary boundary layer parameterization schemes and their sensitivity in simulating southeastern U.S. cold season severe weather environments. *Weather Forecast.* 30, 591–612.
- Estoque, M.A., Bhumralkar, C.M., 1970. A method for resolving the planetary boundary-layer equations. *Bound.-Layer Meteorol.* 1 (2), 169–194.
- Fast, J.D., Gustafson, W.I., Easter, R.C., Zaveri, R.A., Barnard, J.C., Chapman, E.G., Grell, G.A., Peckham, S.E., 2006. Evolution of ozone, particulates, and aerosol direct radiative forcing in the vicinity of Houston using a fully coupled meteorology-chemistry-aerosol model. *J. Geophys. Res.* 111, D21305.
- Fountoukis, C., Ayoub, M.A., Ackermann, L., Perez-Astudillo, D., Bachour, D., Gladich, I., Hoehn, R.D., 2018. Vertical ozone concentration profiles in the Arabian Gulf region during summer and winter: sensitivity of WRF-Chem to planetary boundary layer schemes. *Aerosol Air Qual. Res.* 18, 1183–1197.
- Garratt, J., 1994. The atmospheric boundary layer. Cambridge Atmospheric and Space Science Series.
- Grachev, A.A., Andreas, E.L., Fairall, C.W., Guest, P.S., Persson, P.O.G., 2007. SHEBA flux-profile relationships in the stable atmospheric boundary-layer. *Bound.-Layer Meteorol.* 124 (3), 315–333.
- Grell, G.A., Peckham, S.E., Schmitz, R., McKeen, S.A., Frost, G., Skamarock, W.C., Eder, B., 2005. Fully coupled “online” chemistry within the WRF model. *Atmos. Environ.* 39, 6957–6975.
- Ha, K.J., Mahrt, L., 2001. Simple inclusion of z-less turbulence within and above the modeled nocturnal boundary layer. *Mon. Weather Rev.* 129, 2136–2143.
- Han, Z., Sakurai, T., Ueda, H., Carmichael, G.R., Streets, D., Hayami, H., Wang, Z., Holloway, T., Engardt, M., Hozumi, Y., Park, S.U., Kajino, M., Sartelet, K., Fung, C., Bennet, C., Thongboonchoo, N., Tang, Y., Chang, A., Matsuda, K., Amann, M., 2008. Model intercomparison and evaluation of ozone and relevant species – MICS-Asia. *Atmos. Environ.* 42, 3491–3509.
- Han, S.Q., Liu, J.L., Hao, T.Y., Zhang, Y.F., Li, P.Y., Yang, J.B., Wang, Q.L., Cai, Z.Y., Yao, Q., Zhang, M., Wang, X.J., 2018. Boundary layer structure and scavenging effect during a typical winter haze-fog episode in a core city of BTH region, China. *Atmos. Environ.* 179, 187–200.
- Hong, S.Y., Noh, Y., Dudhia, J., 2006. A new vertical diffusion package with explicit treatment of entrainment processes. *Mon. Weather Rev.* 134, 2318–2341.
- Hu, X.M., Nielsen-Gammon, J.W., Zhang, F.Q., 2010. Evaluation of three planetary boundary layer schemes in the WRF model. *J. Appl. Meteorol. Climatol.* 49, 1831–1844.
- Hu, X.M., Klein, P.M., Xue, M., 2013. Evaluation of the updated YSU planetary boundary layer scheme within WRF for wind resource and air quality assessments. *J. Geophys. Res. Atmos.* 118, 10490–10505.
- Jahn, D.E., Takle, E.S., Gallus, W.A., 2017. Improving wind-ramp forecasts in the stable boundary layer. *Bound.-Layer Meteorol.* 163, 423–446.
- Janjic, Z., 2002. Nonsingular implementation of the Mellor-Yamada level 2.5 scheme in the NCEP MESO model. *NCEP Office Note.* 437, p. 61.
- Kim, J.W., Mahrt, L., 1992. Simple formulation of turbulent mixing in the stable free atmosphere and nocturnal boundary-layer. *Tellus A* 44 (5), 381–394.
- Lee, X., Gao, Z.Q., Zhang, C.L., Chen, F., Hu, Y.Q., Jiang, W.M., Liu, S.H., Lu, L.H., Sun, J.L., Wang, J.M., Zeng, Z.H., Zhang, Q., Zhao, M., Zhou, M.Y., 2015. Priorities for boundary-layer meteorology research in China. *Bull. Amer. Meteorol. Soc.* 96, 149–151.
- Li, D., 2019. Turbulent Prandtl number in the atmospheric boundary layer - where are we now? *Atmos. Res.* 216, 86–105.
- Li, Y., An, J.L., Min, M., Zhang, W., Wang, F., Xie, P.H., 2011. Impacts of HONO sources on the air quality in Beijing, Tianjin and Hebei province of China. *Atmos. Environ.* 45, 4735–4744.
- Li, T., Wang, H., Zhao, T.L., Xue, M., Wang, Y.Q., Che, H.Z., Jiang, C., 2016. The impacts of different PBL schemes on the simulation of PM_{2.5} during severe haze episodes in the Jing-Jin-Ji region and its surroundings in China. *Adv. Meteorol.* 2016, 1–15.
- Madala, S., Satyanarayana, A.N.V., Srinivas, C.V., Kumar, M., 2015. Mesoscale atmospheric flow-field simulations for air quality modeling over complex terrain region of Ranchi in eastern India using WRF. *Atmos. Environ.* 107, 315–328.
- Mellor, G.L., Yamada, T., 1982. Development of a turbulence closure model for geophysical fluid problems. *Rev. Geophys.* 20, 851–875.
- Mohan, M., Gupta, M., 2018. Sensitivity of PBL parameterizations on PM10 and ozone simulation using chemical transport model WRF-Chem over a sub-tropical urban airshed in India. *Atmos. Environ.* 185, 53–63.
- Munoz-Esparza, D., Sharman, R.D., 2018. Turbulence dissipation rate in the atmospheric boundary layer: observations and WRF modeling during the XPIA field campaign. *Mon. Weather Rev.* 146, 351–371.

- Nakanishi, M., Niino, H., 2006. An improved Mellor-Yamada level-3 model: its numerical stability and application to a regional prediction of advection fog. *Bound.-Layer Meteorol.* 119 (2), 397–407.
- Nielsen-Gammon, J.W., Hu, X.M., Zhang, F.Q., Pleim, J.E., 2010. Evaluation of planetary boundary layer scheme sensitivities for the purpose of parameter estimation. *Mon. Weather Rev.* 138, 3400–3417.
- Noh, Y., Cheon, W.G., Hong, S.Y., Raasch, S., 2003. Improvement of the K-profile model for the planetary boundary layer based on large eddy simulation data. *Bound.-Layer Meteorol.* 107 (2), 401–427.
- Parra, R., 2019. Performance studies of planetary boundary layer schemes in WRF-Chem for the Andean region of Southern Ecuador. *Atmos. Pollut. Res.* 9 (3), 411–428.
- Pleim, J.E., 2007. A combined local and nonlocal closure model for the atmospheric boundary layer. Part I: model description and testing. *J. Appl. Meteor. Climatol.* 46, 1383–1395.
- Qi, J., Zheng, B., Li, M., Yu, F., Chen, C.C., Liu, F., Zhou, X.F., Yuan, J., Zhang, Q., He, K.B., 2017. A high-resolution air pollutants emission inventory in 2013 for the Beijing-Tianjin-Hebei region, China. *Atmos. Environ.* 170, 156–168.
- Roman-Cascon, C., Yague, C., Sastre, M., Maqueda, G., Salamanca, F., Viana, S., 2012. Observation and WRF simulations of fog events at the Spanish Northern Plateau. *Adv. Sci. Res.* 8 (1), 11–18.
- Ruiz, J.J., Saulo, C., Nogues-Paegele, J., 2010. WRF model sensitivity to choice of parameterization over South America: validation against surface variables. *Mon. Weather Rev.* 138, 3342–3355.
- Sathyamadh, A., Prabha, T.V., Balaji, B., Resmi, E.A., Karipot, A., 2017. Evaluation of WRF PBL parameterization schemes against direct observations during a dry event over the Ganges valley. *Atmos. Res.* 193, 125–141.
- Schell, B., Ackermann, I.J., Hass, H., Binkowski, F.S., Ebel, A., 2001. Modeling the formation of secondary organic aerosol within a comprehensive air quality model system. *J. Geophys. Res.* 106, 28275–28293.
- Schlichting, H., 1979. Boundary-Layer Theory. 7th ed. McGraw-Hill Higher Education, New York, pp. 705–708.
- Schumann, U., Gerz, T., 1995. Turbulent mixing in stably stratified flows. *J. Appl. Meteorol.* 34 (1), 33–48.
- Steeneveld, G., Ronda, R., Holtslag, A., 2015. The challenge of forecasting the onset and development of radiation fog using mesoscale atmospheric models. *Bound.-Layer Meteorol.* 154 (2), 265–289.
- Stockwell, W.R., Middleton, P., Chang, J.S., Tang, X.Y., 1990. The second generation regional acid deposition model chemical mechanism for regional air quality modeling. *J. Geophys. Res.* 95, 16343–16367.
- Tian, Y.Z., Shi, G.L., Han, S.Q., Zhang, Y.F., Feng, Y.C., Liu, G.R., Gao, L.J., Wu, J.H., Zhu, T., 2013. Vertical characteristics of levels and potential sources of water-soluble ions in PM10 in a Chinese megacity. *Sci. Total Environ.* 447C (49), 1–9.
- Tie, X.X., Geng, F., Guenther, A., Cao, J., Greenberg, J., Zhang, R., Apel, E., Li, G., Weinheimer, A., Chen, J., Cai, C., 2013. Megacity impacts on regional ozone formation: observations and WRF-Chem modeling for the MIRAGE-Shanghai field campaign. *Atmos. Chem. Phys.* 13, 5655–5669.
- Tymvios, F., Charalambous, D., Michaelides, S., Lelieveld, J., 2018. Intercomparison of boundary layer parameterizations for summer conditions in the eastern Mediterranean island of Cyprus using the WRF-ARW model. *Atmos. Res.* 208, 45–59.
- Wang, H., Peng, Y., Zhang, X.Y., Liu, H.L., Zhang, M., Che, H.Z., Cheng, Y.L., Zheng, Y., 2018. Contributions to the explosive growth of PM_{2.5} mass due to aerosol-radiation feedback and decrease in turbulent diffusion during a red alert heavy haze in Beijing-Tianjin-Hebei, China. *Atmos. Chem. Phys.* 18, 17717–17733.
- Xie, B., Fung, C.H., Chan, A., Lau, A., 2012. Evaluation of nonlocal and local planetary boundary layer schemes in the WRF model. *J. Geophys. Res.* 117, D12103.
- Xu, H.Y., Zhai, G.Q., Wang, D.H., Shen, H.F., Liu, R., 2015. An evaluation of the Mellor-Yamada-Janjic formulation parameters for the QNSE scheme in the WRF model over the Lower Yangtze River Valley. *Terr. Atmos. Ocean. Sci.* 26 (3), 283–299.
- Yang, J.B., Liu, J.L., Han, S.Q., Yao, Q., Cai, Z.Y., 2019. Study of the meteorological influence on ozone in urban areas and their use in assessing ozone trends in all seasons from 2009 to 2015 in Tianjin, China. *Meteorol. Atmos. Phys.* 131 (6), 1661–1675.
- Zhang, Y.F., Xu, H., Shi, Y.Z., Zeng, F., Wu, J.H., Zhang, X.Y., Li, X., Zhu, T., Feng, Y.C., 2011. The study on vertical variability of PM10 and the possible sources on a 220m tower in Tianjin, China. *Atmos. Environ.* 45 (34), 6133–6140.
- Zheng, G.J., Duan, F.K., Ma, Y.L., Zhang, Q., Huang, T., Kimoto, T., Cheng, Y.F., Su, H., He, K.B., 2016. Episode-based evolution pattern analysis of haze pollution: method development and results from Beijing, China. *Environ. Sci. Technol.* 50, 4632–4641.